

# TIME EXTENDED PRODUCTION OF NEUTRONS DURING A SOLAR FLARE

Chupp, E. L., Forrest, D. J., Vestrand, W. T.  
University of New Hampshire, Durham, NH 03824, USA

Debrunner, H., Flückiger, E.  
Universität Bern, Bern, Switzerland

Cooper, J. F., Kanbach, G., Reppin, C.  
Max-Planck-Institute für extraterrestrische Physik, 8046 Garching, FRG

Share, G. H.  
E.O. Hulburt Center for Space Research, Naval Research Laboratory,  
Washington, D.C. 20375, USA

**1. Introduction.** The most energetic neutral emissions expected from solar flares are  $\gamma$ -rays ( $>10$  MeV) from relativistic primary and secondary electron bremsstrahlung, from  $\pi^0$  meson decay, and from neutrons ( $>50$  MeV). Bremsstrahlung photon energies extend to that of the highest energy electron present, but the shape of the  $\pi^0$   $\gamma$ -ray spectrum, peaking at 69 MeV, does not depend strongly on the proton spectrum above threshold, which is  $\sim 292$  MeV for meson production on protons. The highest energy neutrons observed indicate directly the highest energy ions which interact at the Sun, and the presence or absence of an energy cutoff in the acceleration process. The high-energy proton spectrum shape can be determined from the neutron spectrum.

Detection of solar neutrons at the Earth with energies from 10 MeV to 1000 MeV have been reported from observations by the Gamma-Ray Spectrometer (GRS) on the Solar Maximum Mission (SMM) satellite (1,2), and from ground level neutron monitors (3), and through observations of the neutron-decay protons (4,5,6). By the use of new Monte Carlo calculations of the neutron and  $\gamma$ -ray responses of the SMM GRS (7) we have reevaluated the GRS neutron observations taking into account the effect of continuous production of rays and neutrons. This analysis has been carried out for two intense major solar flares; on 1980 June 21 and 1982 June 3, hereafter referred to as event I and II. The  $\gamma$ -ray results are given in (8). We find that the revised neutron efficiencies and background determination require some modification of the neutron results reported for event I (1). We also find that when continuous production of neutrons is taken into account that previous interpretation regarding event II must be revised (2,3).

**2. Methods.** We first reestablish that the SMM GRS high-energy detector has detected a neutron flux in the delayed phase of the 1980 June 21 impulsive limb flare. The high-energy detector portion in the SMM GRS, described in (9), consists of the 7 NaI elements and a single 24 cm X 7.5 cm CsI element, and records energy loss events in all elements, in 4 windows between 10 MeV and 100 MeV. In Figure 1 we show the excess GRS count rate in high-energy elements for energy losses  $> 10$  MeV. These excess rates are averaged over 65.54 s and are found by subtracting a measured background from the total GRS counts obtained during the flare. The principal characteristic in this plot is that the high-energy excess count rate rises steadily after the impulsive phase has fully terminated at 0122 UT. Since there is an absence of excess counts after this time at all energy losses ( $< 10$  MeV), we

attribute these excess counts to the arrival of solar neutrons at the SMM GRS. If a short burst of neutrons were released at the Sun during the impulsive phase, the count rate grows with time as progressively lower energy neutrons arrive at the Earth. This interpretation is the same as given earlier for this event (1) but we can now compare the GRS observations with the results of the Monte Carlo calculations of the GRS response (7), which predict that energy loss events due to high-energy neutrons should be confined to individual detector elements rather than produce simultaneous losses in both NaI and CsI. On the other hand, any  $\gamma$ -ray spectrum will produce a significant fraction of "mixed" events; that is, energy loss in both the NaI and CsI detector elements.

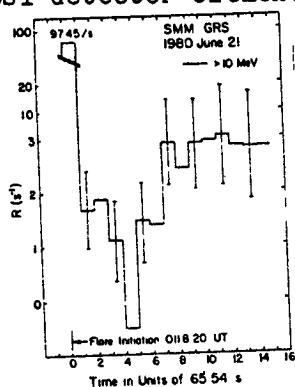


Fig. 1. GRS High-Energy detector average excess count rate during and after the impulsive limb flare at 0118.20 UT on 1980 June 21. The main impulsive phase at all energies occurs within the first time interval indicated but extends for about 3 minutes for all events  $> 10$  MeV. The neutron event commences in interval 5. SMM GRS

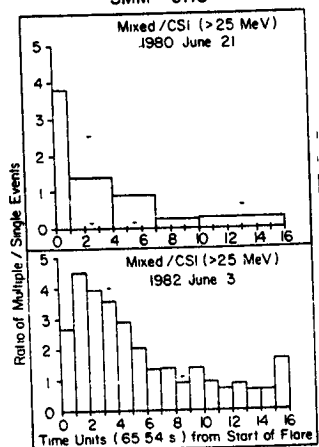


Fig. 2. The observed ratio of multiple events (NaI and CsI) to single events (CsI) for events I and II as a function of time during each event.

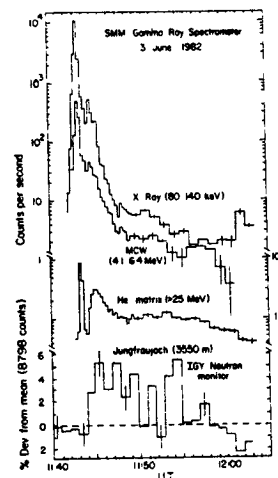


Fig. 3. The time histories for several GRS data channels are shown for the 1982 June 3 flare (event II) at 1143 UT and the corresponding response from the Jungfraujoch neutron monitor.

In Figure 2 we show, for events I and II, the observed behavior of the ratio of "mixed" high-energy events to those in the CsI element alone (above 25 MeV energy loss) from the impulsive phase until the end of the daylight portion of the flare orbit. During event I this ratio is initially about (0.3-0.4), but during the delayed phase it falls to  $0.047 \pm 0.023$  when averaged over a full 10 minutes of delayed emission. For a spectrum due only to  $\pi^0$   $\gamma$  rays and the associated meson decay electron bremsstrahlung, this ratio is expected to be rather large, 0.5-0.6, while primary electron bremsstrahlung spectra give a ratio ranging from 0.4-0.1 for power laws with exponents 1 to 5, respectively. As mentioned above, Monte Carlo calculations show this ratio is essentially zero for a pure flux of neutrons, and we conclude that the neutron interpretation for the delayed phase of event I is valid. No other reasonable explanation has been found for the delayed emission in this event.

**3. Results.** Observations of solar neutrons at the Earth were first reported for event II on 1982 June 3 from neutron-decay proton observations (4). Further reports came from GRS observations (2), and from ground level neutron monitors (3). In Figure 3 we show the count rate time histories for several GRS data channels, and for the Jungfraujoch neutron monitor which has a one minute sampling time.

It has been previously reported (3) that

the Jungfraujoch neutron monitor recorded high-energy neutrons in the time interval  $> (1144-1155)$  UT. Two other European neutron monitors, at Lominicky Stit and Rome, also recorded simultaneous increases, averaged over five minutes. Since the neutron monitors have an efficiency that increases continuously above 300 MeV but falls sharply below this energy, the early response of the Jungfraujoch monitor at 1144-1145 UT must be due to neutrons of GeV energy, if they were produced at the Sun at the time of the impulsive 1143 UT  $\gamma$ -ray peak shown in Figure 3. It should be noted that the neutron monitor response (Figure 3) above background, continues until  $\sim 1155$  UT. This observation requires that significant production of high-energy neutrons ( $> 300$  MeV) at the Sun must have continued well after the initial impulsive burst, since arriving neutrons from this emission would have energies well below that required to develop a significantly large atmospheric nucleon cascade (10).

In the case of the GRS rates, during event II the ratio of "mixed" to single events is initially large ( $\sim 0.4$ ) and falls to  $\sim 0.1$  at  $\sim 1149$  UT (Figure 2). Based on the GRS response to neutrons in event I, and assuming that the Monte Carlo calculations are correct in predicting no "mixed" events for neutrons, we would conclude that the GRS is responding to a combined flux of photons and neutrons. This circumstance alone indicates that photon production also continues throughout the post-impulsive phase. Earlier it was suggested (2) that the GRS was responding to a combined flux of  $\gamma$ -rays and neutrons between 1144-1147 UT, and that from 1147-1206 UT the energy loss spectrum was basically characteristic of high-energy neutron interactions in the GRS scintillators. We must now reevaluate the earlier conclusions on neutron observations in event II using a model for combined high-energy photon and neutron production throughout the event.

We have used several approaches to study the neutron and  $\gamma$ -ray contributions to the GRS rates in the post-impulsive phase. One approach assumes that  $\gamma$ -ray and neutron production rates are proportional throughout the flare and that spectral shapes do not change with time. Using this assumption, and  $\pi^0$  fluence versus time, (8), we can test any assumed neutron spectrum against the Jungfraujoch and GRS data. As an example we have used a neutron production spectrum at the Sun (11), based on a Bessel function accelerated proton spectrum (parameter  $\alpha T$ ). To perform this test we calculate the expected unnormalized count rate of the Jungfraujoch neutron monitor versus time using its known neutron sensitivity (3). This rate is then normalized to the observed monitor rates (Figure 3) by a  $\chi^2$  minimization for a given neutron production spectrum. Each best fit absolute continuous production solar neutron spectrum shape is then used to predict the GRS count rate versus time using the Monte Carlo results for the GRS sensitivity. Because of the limited statistics of the 1 minute neutron monitor rates, the normalization of the predicted curves is not better than a factor of 2.

Figure 4 shows a comparison of the predicted GRS count rate versus time for  $\alpha T = 0.03$  and  $0.05$ , compared with the GRS total high-energy detector rates averaged over 65.54 sec. Calculations of predicted rates for other  $\alpha T$  spectral shapes are in progress.

**4. Discussion** We have confirmed that the delayed emission observed by the GRS in event I is due to neutrons with energies from 50 MeV to  $> 250$  MeV,

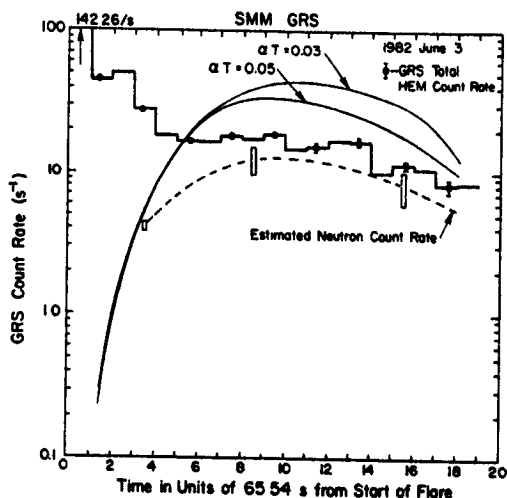


Fig. 4. The total GRS high-energy count rates for energy loss  $> 10$  MeV compared with predicted  $\alpha T$  fits determined from a time extended production of neutrons and normalized to Jungfraujoch neutron monitor rates. The estimated neutron count rate (dashed) is based on subtracting meson  $\gamma$ -ray contributions from the total rate (8). Error ranges are  $1\sigma$  - count statistics only.

assuming a delta function emission of neutrons at the Sun. Over this limited energy range, a neutron spectrum at the Sun of power law form ( $\alpha = 3.6$ ), or that produced by a proton Bessel function spectrum ( $\alpha T = 0.02$ ) is sufficient to fit the observed neutron flux at the Earth. This result is not changed significantly if the neutron emission is spread over the short time interval of the impulsive emission (1).

In the case of event II, we have confirmed that a time extended production of neutrons at the Sun is required to account for the response of the GRS and the Jungfraujoch neutron monitor throughout the delayed phase. Therefore a delta function production in the impulsive phase cannot account for the observations of the neutron monitors and the GRS to solar neutrons. As a consequence there is not a one to one

correspondence of arrival time to neutron energy, and this complicates the determination of a neutron spectrum. Also, a neutron production spectrum at the Sun resulting from a Bessel function flatter than  $\alpha T = 0.05$  may be required to pull the predicted neutron count ratio down to that required for the GRS simultaneous response to both neutrons and  $\gamma$  rays. This is indicated by the dashed curve in Figure 4. As previously pointed out (11, 12) a power-law spectral shape which is constant from 1 GeV down to 50 MeV is not viable.

**5. Conclusions.** Reanalysis of the GRS neutron observations taking into account time extended production of  $\gamma$  rays and neutrons and the neutron monitor results has led to a reinterpretation of event II. Theoretical results we have used here had assumed isotropic production of neutrons and an invariant spectral shape with time. It may be necessary to consider the effects of nonisotropic neutron production and a time varying spectral shape to satisfy all observational constraints including those provided by the neutron-decay protons.

**6. Acknowledgements.** We wish to thank Mary Chupp for and Robin Tuttle for preparation of this manuscript; Karen Dowd, Sabrina Kirwan, and Bao Li for data analysis assistance. This work was partially supported by contract NAS 5-28609 at the University of New Hampshire; NASA contract S.70926A at NRL; contract 010K017ZA/WS/WRK 0275:4 at the MPI, FRG; and the Swiss National Science Foundation Grant 2.876.80 at the U. of Bern.

#### References

1. Chupp, E. L., et al. (1982) Ap. J. (Letters) 263, L95.
2. Chupp, E. L., et al. (1983) Proc. 18th ICRC, 10, 33.
3. Debrunner, H., et al. (1983) Proc. 18th ICRC, 1, 75.
4. Evenson, P., et al. (1983) Ap. J. 274, 875.
5. Evenson, P., et al. (1983) Proc. 18th ICRC, 4, 97.
6. Meyer, P., et al. (1985) Bull. Am. Phys. Soc. 30, 780.
7. Cooper, J. F., et al. (1985) This Conference SH 9.1, 1.
8. Forrest, D. J., et al. (1985) This Conference SH 1.4-7
9. Forrest, D. J., et al. (1980) Solar Physics 65, 15.
10. Debrunner, H., et al. (1984), Presented at the 9th European Cosmic Ray Symposium, Kosice.
11. Murphy, R. J. and Ramaty, R., (1985) Advances in Space Research 4, 127.
12. Ramaty, R., et al. (1983), Solar Physics 86, 395.